Assessment of non-prismatic beams having symmetrical parabolic haunches with constant haunch length ratio of 0.5

S. Bahadir Yuksel*

Department of Civil Engineering, Selcuk University, Konya 42075, Turkey

Abstract. Single span historic bridges often contain non-prismatic members identified with a varying depth along their span lengths. Commonly, the symmetric parabolic height variations having the constant haunch length ratio of 0.5 have been selected to lower the stresses at the high bending moment points and to maintain the deflections within the acceptable limits. Due to their non-prismatic geometrical configuration, their assessment, particularly the computation of fixed-end horizontal forces (FEFs) and fixed-end moments (FEMs) becomes a complex problem. Therefore, this study aimed to investigate the behavior of non-prismatic beams with symmetrical parabolic haunches (NBSPH) having the constant haunch length ratio of 0.5 using finite element analyses (FEA). FEFs and FEMs due to vertical loadings as well as the stiffness coefficients and the carry-over factors were computed through a comprehensive parametric study using FEA. It was demonstrated that the conventional methods using frame elements can lead to significant errors, and the deviations can reach to unacceptable levels for these types of structures. Despite the robustness of FEA, the generation of FEFs and FEMs using the nodal outputs of the detailed finite element mesh still remains an intricate task. Therefore, this study advances to propose effective formulas and dimensionless estimation coefficients to predict the FEFs, FEMs, stiffness coefficients and carry-over factors with reasonable accuracy for the analysis and re-evaluation of the NBSPH. Using the proposed approach, the fixed-end reactions due to vertical loads, and also the stiffness coefficients and the carry-over factors of the NBSPH can be determined without necessitating the detailed FEA.

Keywords: historic bridge; non-prismatic member; finite element analysis; parabolic haunch; stiffness factor; fixed-end reactions

1. Introduction

The girders used for the long spans of the bridges and the buildings are designed to be non-prismatic by means of variable depth along the span length. Variable depth variations are commonly preferred to lower the stresses at the high bending moment regions and to maintain the deflections within acceptable limits. The non-prismatic structural members commonly have haunches, which can be stepped, tapered, or in parabolic shape. As depicted in Fig. 1, in general, the single span reinforced concrete historic bridges have symmetrical parabolic haunches with the constant haunch

---

*Corresponding author, Professor, E-mail: sbahadiryuksel@yahoo.com
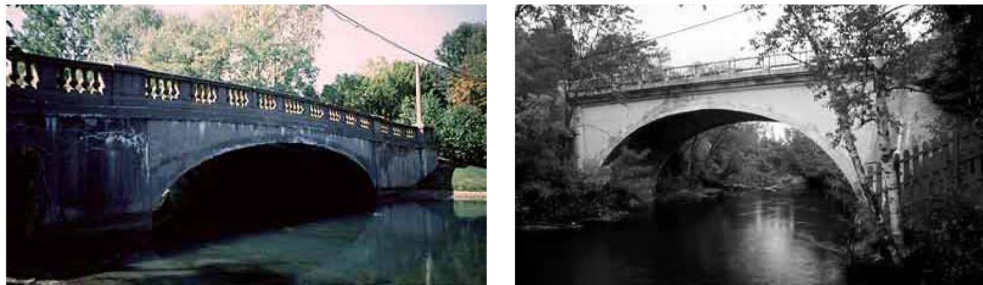
Fig. 1 Typical single span reinforced concrete historic bridges with symmetrical parabolic haunches having the constant haunch length ratio of 0.5
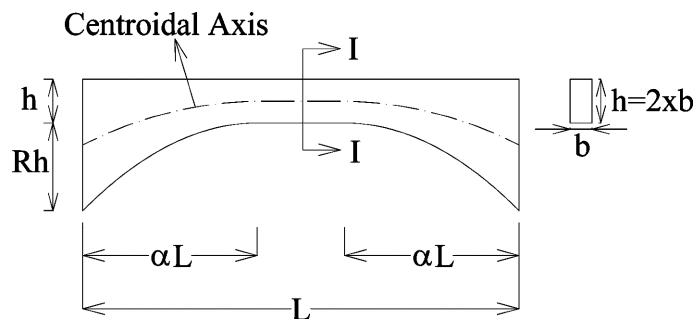

Fig. 2 Geometric parameters of the typical non-prismatic beams having symmetric parabolic haunches

length ratio (α) of 0.5 but varying haunch depth ratios (R) (see Fig. 2 for detailed description of α and R).

Due to their non-prismatic geometrical configuration, the analysis and re-evaluation of the NBSPH, particularly the computation of FEFs and FEMs becomes a difficult task. Different approaches were proposed for the analysis of non-prismatic members in the literature. In 1958, Portland Cement Association issued the "Handbook of Frame Constants (PCA 1958) including a series of tables containing stiffness coefficients, carry-over factors and FEM coefficients for commonly used non-prismatic members. Despite the crude assumptions embedded in PCA methodologies, these stiffness coefficients, carry-over factors and FEM coefficients have still been used in conventional methods since 1958 for the analyses of non-prismatic members (Maugh 1964, Timoshenko and Young 1965, Tartaglione 1991, Hibbeler 2002) while utilizing the moment distribution, slope deflection and the matrix displacement methods.

The elastic modeling of the non-prismatic members evolved after the publication of the PCA handbook of the frame constants (PCA 1958) and caught the attention of a few researchers in the last four decades (Tena-Colunga 1996). Medwadowski (1984) solved the bending problem of the non-prismatic shear beams in terms of a displacement function, which is based on the calculus of variations. Vanderbilt (1978), Funk and Wang (1988) calculated the stiffness matrix and fixed-end forces by dividing the non-prismatic member into sub-elements. Brown (1984) presented a method in which the approximate interpolation functions consistent with the beam theory and the virtual work principle are used to obtain the stiffness matrix for tapered beams. Eisenberger (1985, 1991), Friedman and Kosmatka (1992a, b) derived stiffness matrices for members having linear and

parabolic variations using beam theories. Al-Gahtani (1996) derived the stiffness matrix by using differential equations and the boundary integral method, and determined fixed-end forces for distributed and concentrated member loads. Tena-Colunga (1996) derived the stiffness matrix for linearly tapered members with rectangular, circular, and square cross sections, while accounting for shear deformations. In all of the references cited above, the analysis is based on the formulas derived for prismatic members where the centroidal axis is a straight line, while in non-prismatic members either the axis or its slope is discontinuous. Based on FEA results, El Mezaini *et al.* (1991), Balkaya (2001), Yuksel (2009a) proved that the conventional solution techniques of the non-prismatic structures lead to erroneous results and the deviations reach to unacceptable levels for these types of structures especially with deep haunches. Because of arching action in non-prismatic members, the change or discontinuity of the centroidal axis produces axial forces under vertical loadings when the ends of non-prismatic members are restrained. This creates a coupling between the bending moments and axial forces. Unless the detailed finite element modeling is utilized, the conventional methods using frame elements become deficient in computing correct member forces due to progressive change in centroidal axis associated with the non-prismatic sections.

The objective of this study is to investigate the behavior of the non-prismatic beams with symmetrical parabolic haunches having constant haunch length ratios of $\alpha = 0.5$. In this conjunction, the present study carried out many FEA for various NBSPH. To produce benchmark results for the FEA, four-node isoparametric plane-stress finite elements with two translational degrees of freedom and one rotational degree of freedom per node were utilized for modeling various non-prismatic beams. FEFs and FEMs due to vertical loadings as well as stiffness coefficients and carry-over factors were computed by varying the depths of the haunches. Alternatively, the design formulas and the dimensionless estimation coefficients were proposed based on the comprehensive parametric study using two-dimensional plane-stress FEA. Using the proposed approach, the evaluation of NBSPH can be achieved without necessitating detailed FEA. Additionally, the robust results of FEA allowed examining the sources and magnitudes of the errors in the conventional frame analysis.

2. Assumptions for the development of the analytical model and the parametric study

The non-prismatic beams having symmetric parabolic variable depths with haunch length ratios of $\alpha = 0.5$ were generated as the model structures of the analysis. The geometric parameters of the typical NBSPH are presented in Fig. 2; where, L is the span length, b is the width, h is the mid-span depth or the smallest depth, α is the haunch length ratio (haunch length divided by the total length of the member) and R is the haunch depth ratio. In all of the analyses, the beam lengths ($L =$ 10 m), the beam widths ($b = 0.5$ m) and the mid-span depths ($h = 1$ m) of the non-prismatic elements were taken as constant while the other values were changed to achieve the parameter values. The non-prismatic beam members of rectangular cross section ($b \times h$) and length L were assumed to be made up of homogeneous, isotropic and linearly elastic material. The modulus of elasticity (E) and the Poisson's ratio (ν) were taken as 3×10^7 kN/m^2 and 0.2, respectively. The single span reinforced concrete historic bridges were commonly constructed with the haunch length ratio of $\alpha = 0.5$ with rectangular cross-section, but they have different haunch depth ratios. For that reason, to be able to simulate the behavior of the single span reinforced concrete historic bridges, the parametric studies were performed considering a constant haunch length ratio of $\alpha = 0.5$ with
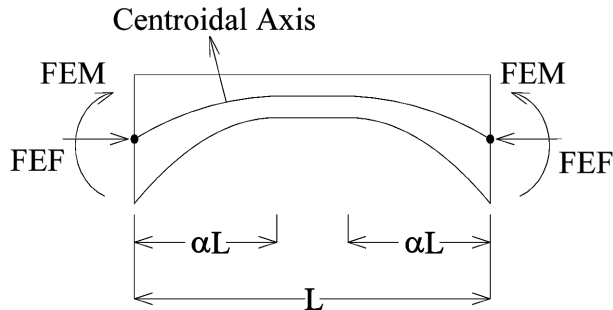
Fig. 3 Fixed-end reactions at the ends of the non-prismatic beams having symmetric parabolic haunches

varying R in the range of 0.0 to 4.0 with 0.1 increments. The combination of all these values resulted in 40 NBSPH different from each other in geometry. In all of the cases, the effects of shear deformations were considered, and the fixed-end conditions were assumed at the supports. The NBSPH having deep haunches undergo significant shear deformations. Thus, the effect of shear deformation in the NBSPH having deep haunches is of greater importance than in conventional prismatic beams. Consequently, the effect of shear deformations was taken into account in deriving the fixed-end reactions, stiffness coefficients and carry-over factors of the NBSPH.

The NBSPH are submitted to static-elastic analysis. The applied vertical loads at the top surface occur as the uniformly distributed vertical load ($w = 1$ kN/m^2) and the point load ($P = 10$ kN) at the mid-span of the NBSPH. The point load ($P = 10$ kN) is also applied at $0.3 \times L$ and $0.1 \times L$ from the left end of the NBSPH. In addition to the applied point loads at the top surface, the self weights of the NBSPH were also applied. Fig. 3 illustrates the FEFs and FEMs at the centroids of the end-sections of the NBSPH due to vertical loadings. The FEFs and FEMs of the NBSPH were obtained with the aid of FEA. The results were next used in developing the design equations and the dimensionless estimation coefficients. In addition, FEA are performed to determine the bending stiffness coefficients and the carry-over factors of the NBSPHs. In all the analyses, the effect of shear deformations is also considered.

3. Finite element modeling of the NBSPH

The behavior of the NBSPH was investigated by developing two dimensional finite element models using SAP2000 (CSI 2007). A typical finite element model for the NBSPH with geometrical parameters of $\alpha = 0.5$ and $R = 3$ can be seen in Fig. 4. To produce benchmark results for the FEA, four-node isoparametric plane stress finite elements with two translational degrees of freedom and one rotational degree of freedom per node were utilized for the modeling of various NBSPH. In order to satisfy the adequate accuracy for the results of the FEA, each NBSPH model was sub-divided into 8000 finite elements as shown in Fig. 4. Especially, the modeling of the non-prismatic members with parabolic haunches is complicated by the fact that the bottom face of these members has parabolic shape variations. Most commonly used commercial software (CSI 2007) does not have automated parabolic mesh generation feature. For that reason, a preprocessor was prepared to be able to generate the finite element meshes of the NBSPH.

The results obtained by the FEA can be accepted as the real elastic values. Discontinuity of the
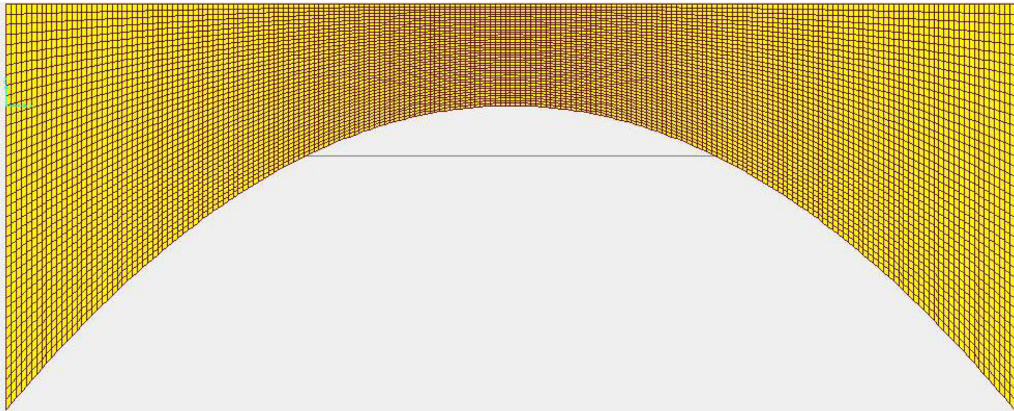
Fig. 4 Typical finite element mesh of the NBSPH having the haunch depth ratio of $R = 3$
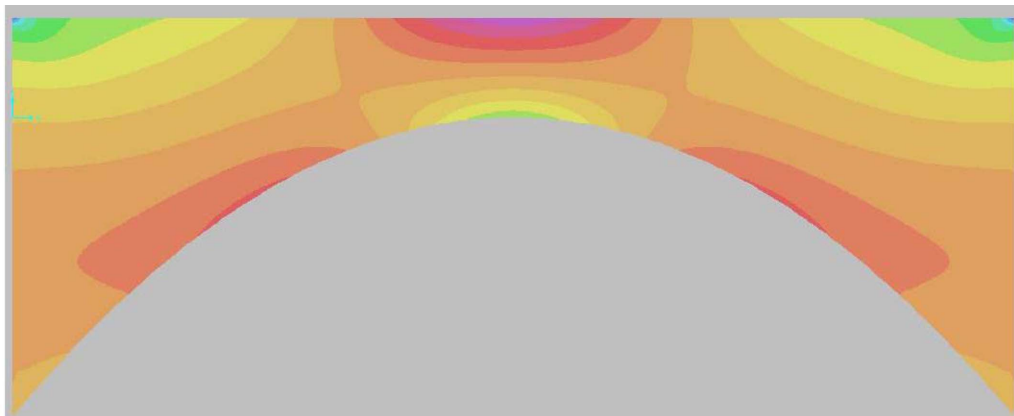

Fig. 5 Axial stress contours obtained by FEA due to the uniformly distributed vertical load of $w = 1$ kN/m

centroidal axis, local stress concentrations, nonlinear stress distributions and existence of null areas that reduces the member stiffness are taken into consideration in finite element models. Since the stress concentrations, non-uniform stress distributions, the coupling between axial forces and moments can not be considered in the classical beam theory, the approximate results obtained from the beam theory deviated from the real elastic values. Fig. 5 shows the axial stress contours of a NBSPH ($R = 3$) due to the uniformly distributed vertical loading of $w = 1$ kN/m in which the maximum stress reaches up to 0.70 kN/m at the mid-span. The stress distributions occurred so complex in the NBSPH subjected to vertical loadings, which require special attention.

The FEFs and FEMs due to vertical loadings as well as the stiffness coefficients and the carry-over factors of the NBSPH were obtained using the FEA. The computation of the stress values or the nodal forces is not sufficient for the calculation of the fixed-end reactions. Despite the robustness of the finite element modeling, the generation of FEFs and FEMs from the nodal outputs of the detailed mesh still remains as an intricate task. The FEFs and FEMs were calculated using the nodal force outputs of the FEA proposed by Bathe (1996) and applied as in the previous finite element studies (Horrowitz 1997, Yuksel 2008, 2009b, c, Yuksel and Arikan 2009). A postprocessor

was developed to sum the element nodal forces at the predetermined sections in order to be able to calculate the fixed-end reactions.

4. End-actions for the restrained non-prismatic members subjected to vertical loadings

A restrained member is the one whose ends are restrained against the translational and rotational displacements, as in the case of a fixed-end beam. Many classical books on structural analysis (Maugh 1964, Timoshenko and Young 1965, Tartaglione 1991, Hibbeler 2002, Weaver and Gere 1990) have given the fixed-end moments reactions for the prismatic and non-prismatic members under vertical loadings. If a prismatic member is subjected to vertical loads, only the FEMs will occur at the ends. However, the FEFs are developed in addition to the FEMs at the ends of the non-prismatic members under vertical loading conditions. The continuous change in the centroidal axis (see Fig. 2) associated with the non-prismatic sections causes a strong coupling between the bending moments and the axial forces.

As shown in Fig. 3, the end reactions for the restrained non-prismatic members subjected to vertical loadings are the reactive actions (FEFs and FEMs) developed at the ends.

The following symbols are used in this paper to be able to distinguish the different types of fixed-end reactions:

FEF = Fixed-end horizontal forces at the centroids of the end sections of the NBSPH due to vertical loadings;

FEM = Fixed-end moments at the centroids of the end sections of the NBSPH due to vertical loadings;

FEF_W = Fixed-end horizontal forces at the centroids of the end sections of the NBSPH due to uniformly distributed vertical loads;

FEM_W = Fixed-end moments at the centroids of the end sections of the NBSPH due to uniformly distributed vertical load;

$FEF_{0.5L-P}$ = Fixed-end horizontal forces at the centroids of the end sections of the NBSPH due to the point loads at the mid-span;

$FEM_{0.5L-P}$ = Fixed-end moments at the centroids of the end sections of the NBSPH due to the point loads at the mid-span;

$FEF_{0.3L-P}$ = Fixed-end horizontal forces at the centroids of the end sections of the NBSPH due to the point load at $0.3 \times L$ from the left end;

$FEM_{0.3L-P-L}$ = Fixed-end moment at the centroid of the left end of the NBSPH due to the point load at $0.3 \times L$ from the left end;

$FEM_{0.3L-P-R}$ = Fixed-end moment at the centroid of the right end of the NBSPH due to the point load at $0.3 \times L$ from the left end;

$FEF_{0.1L-P}$ = Fixed-end horizontal forces at the centroids of the end sections of the NBSPH due to the point load at $0.1 \times L$ from the left end;

$FEM_{0.1L-P-L}$ = Fixed-end moment at the centroid of the left end of the NBSPH due to the point load at $0.1 \times L$ from the left end;

$FEM_{0.1L-P-R}$ = Fixed-end moment at the centroid of the right end of the NBSPH due to the point load at $0.1 \times L$ from the left end;

FEF_{OWN} = Fixed-end horizontal forces at the centroids of the end sections of the NBSPH due

to its own weight;

FEM_{OWN} = Fixed-end moments at the centroids of the end sections of the NBSPH due to its own weight.

5. Evaluation of the FEA results and comparison with the frame element analyses results

The fixed-end forces (FEF_W, $\text{FEF}_{0.5L\text{-}P}$, $\text{FEF}_{0.3L\text{-}P}$, $\text{FEF}_{0.1L\text{-}P}$, FEF_{OWN}), fixed-end moments (FEM_W, $\text{FEM}_{0.5L\text{-}P}$, $\text{FEM}_{0.3L\text{-}P\text{-}L}$, $\text{FEM}_{0.3L\text{-}P\text{-}R}$, $\text{FEM}_{0.1L\text{-}P\text{-}L}$, $\text{FEM}_{0.1L\text{-}P\text{-}R}$, FEM_{OWN}), stiffness coefficients and carry-over factors of the NBSPH were obtained using the FEA. The plots were presented for the variations in the FEFs, FEMs, stiffness coefficients and carry-over factors as the functions of the haunch depth ratios varying in the range of 0.0 to 4.0 with 0.1 intervals ($R = 0.0, 0.1, 0.2, ..., 4.0$).

The results of the FEA performed to investigate the values of FEF_W, $\text{FEF}_{0.5L\text{-}P}$, $\text{FEF}_{0.3L\text{-}P}$, $\text{FEF}_{0.1L\text{-}P}$ and FEF_{OWN} were presented in Fig. 6(a), Fig. 7(a), Fig. 8(a), Fig. 8(b) and Fig. 11(a), respectively. The relationships between the FEFs values and the haunch depth ratios are non-linear. The magnitudes of FEF_W, $\text{FEF}_{0.5L\text{-}P}$, $\text{FEF}_{0.3L\text{-}P}$, $\text{FEF}_{0.1L\text{-}P}$ and FEF_{OWN} increase rapidly with the haunch depth ratios up to a certain limit, and then they start to decrease slightly. It is proven from FEA results that significant amount of horizontal compressive forces occur at the centroids of the end sections of the NBSPH due to vertical loadings. Because of the arching action, the continuous change of the centroidal axis orientation produces FEFs in addition to FEMs under vertical loading conditions, when the ends of the NBSPH are completely restrained. It is obvious that the continuous change of the centroidal axis of the NBSPH cause strong coupling between bending moments and axial forces.

The analytical approaches and the traditional beam theories often need to introduce assumptions to simplify the problem and yield an erroneous solution. Unless a detailed finite element modeling was applied, the conventional methods using frame elements will be deficient in computing these FEFs due to the progressive changes in the centroidal axis of the non-prismatic sections. Since the FEFs values are not available in the literature, the FEFs values obtained from the FEA could not be compared.

NBSPH with small haunch depth ratios, the built-in arch is very shallow so that with a slight axial
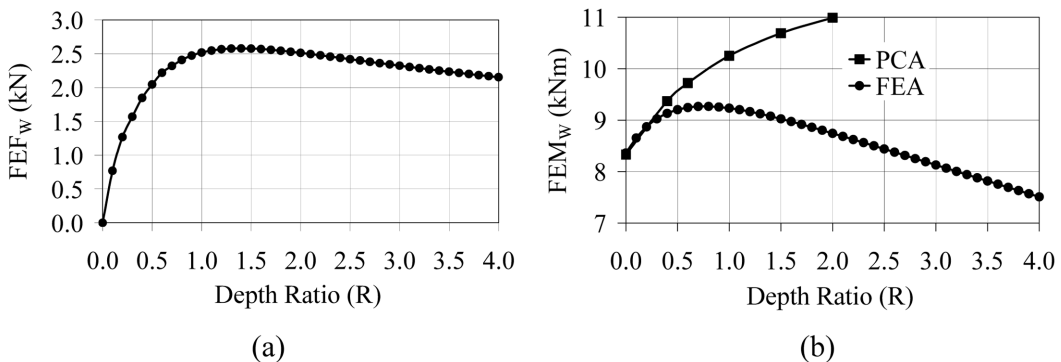

Fig. 6 (a) Variation of FEF_W obtained from FEA, (b) comparison of FEM_W values obtained by the FEA with those of PCA (1958)
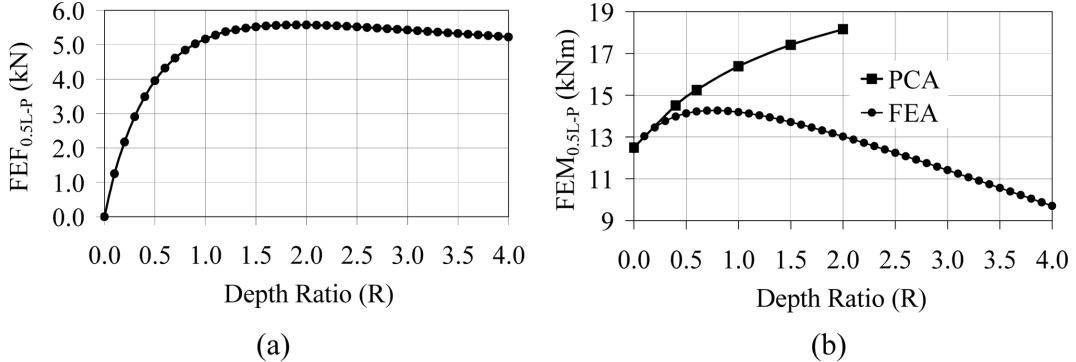
Fig. 7 (a) Variation of $FEF_{0.5L\text{-}P}$ values obtained from FEA, (b) comparison of the $FEM_{0.5L\text{-}P}$ values obtained from FEA with those of PCA (1958)
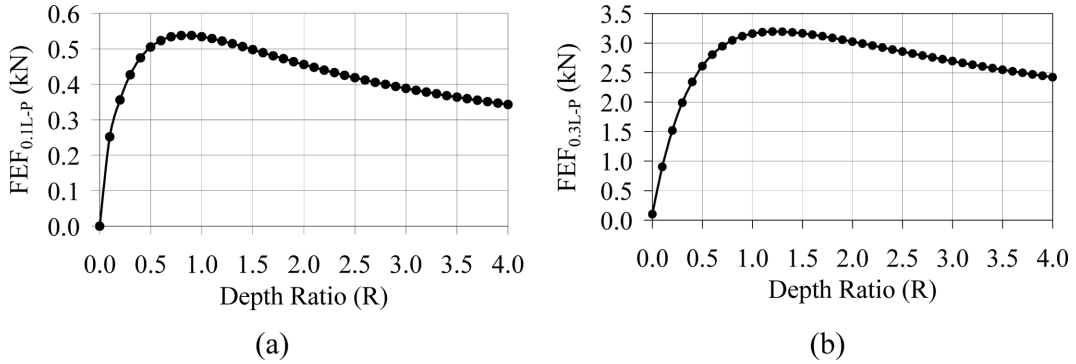
Fig. 8 Variation of (a) $FEF_{0.1L\text{-}P}$, (b) $FEF_{0.3L\text{-}P}$ values obtained from FEA

deformation it will get flat producing a small amount of axial force. NBSPH continues to deform under vertical loadings at the top surface as prismatic beams. As the haunch depth ratio increases, the arch depth increases requiring more axial deformation to get flat, hence, more axial trust is produced. When the arch deep is enough so that it cannot be completed flattened with axial deformations, the horizontal thrust starts to decrease as arch height increases similar to regular arches (El Mezaini *et al.* 1991, Balkaya 2001, Yuksel 2009b, c).

Fig. 6(b) and Fig. 7(b) compare the FEM_W and $FEM_{0.5L\text{-}P}$ values obtained from FEA and those obtained from PCA (1958). The results of the finite element analyses and the frame element analysis were denoted as FEA and PCA (1958), respectively. Note that the values in PCA (1958) are available up to $R = 2$, hence the PCA values end at $R = 2$. The FEM_W and $FEM_{0.5L\text{-}P}$ increase in a parabolic fashion as haunch depths are increased as the classical Bernoulli-Euler beam theory modeling (PCA 1958) is considered; in contrast, the FEM_W and $FEM_{0.5L\text{-}P}$ increase only for the depth ratio of $R = 0.7$ in FEA, and then start to decrease for higher depth ratios. The values of FEM_W and $FEM_{0.5L\text{-}P}$ of the frame element modeling were determined much higher than the FEM_W and $FEM_{0.5L\text{-}P}$ calculated by the FEA for a given haunch depth ratio of R. The deviation in the FEM values increases as the relative haunch depth ratios increase.

$FEM_{0.3L\text{-}P\text{-}L}$, $FEM_{0.3L\text{-}P\text{-}R}$, $FEM_{0.1L\text{-}P\text{-}L}$ and $FEM_{0.1L\text{-}P\text{-}R}$ values obtained from the FEA are compared with the results of the PCA (1958) in Fig. 9(a), Fig. 9(b), Fig. 10(a) and Fig. 10(b), respectively.
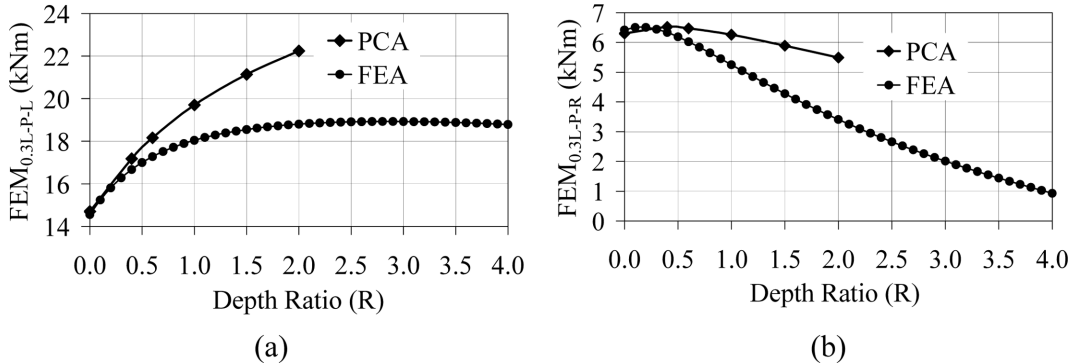
Fig. 9 (a) Comparison of the $FEM_{0.3L-P-L}$ values obtained from FEA with those of PCA (1958), (b) comparison of the $FEM_{0.3L-P-R}$ values obtained from FEA with those of PCA (1958)
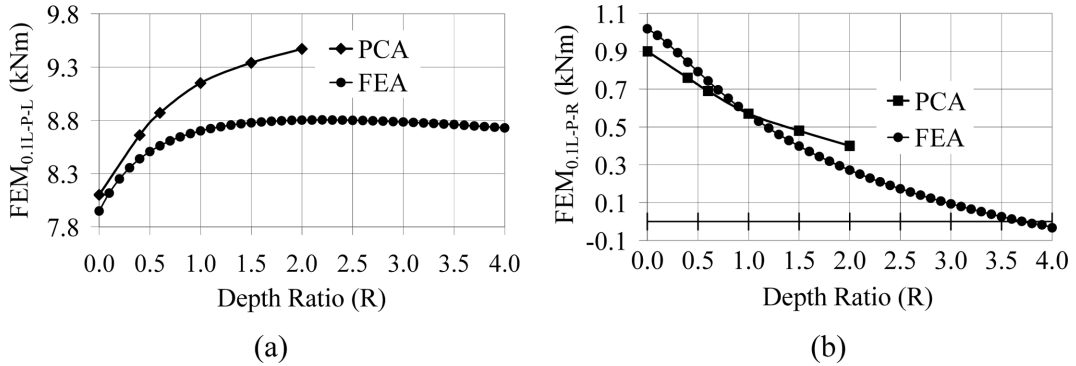
Fig. 10 (a) Comparison of the $FEM_{0.1L-P-L}$ values obtained from FEA with those of PCA (1958), (b) comparison of the $FEM_{0.1L-P-R}$ values obtained from FEA with those of PCA (1958)
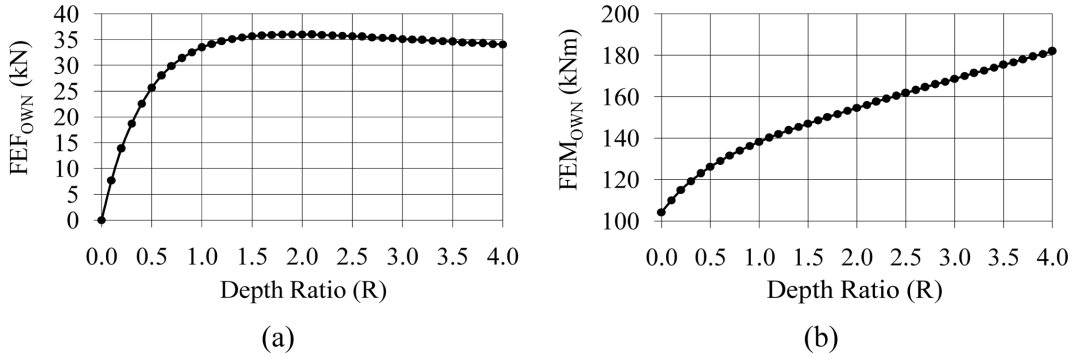
Fig. 11 Variation of (a) FEF_{OWN}, (b) FEM_{OWN} values obtained from FEA

From Fig. 9 and Fig. 10, it can be seen that there are large discrepancies between the results of the two methods of analyses (FEA and PCA 1958). The FEMs of the frame element modeling were determined much higher than the FEMs calculated by the FEA for a given haunch depth ratio. The arching action becomes more important as the haunch depth is increased. Fig. 11(b) shows the
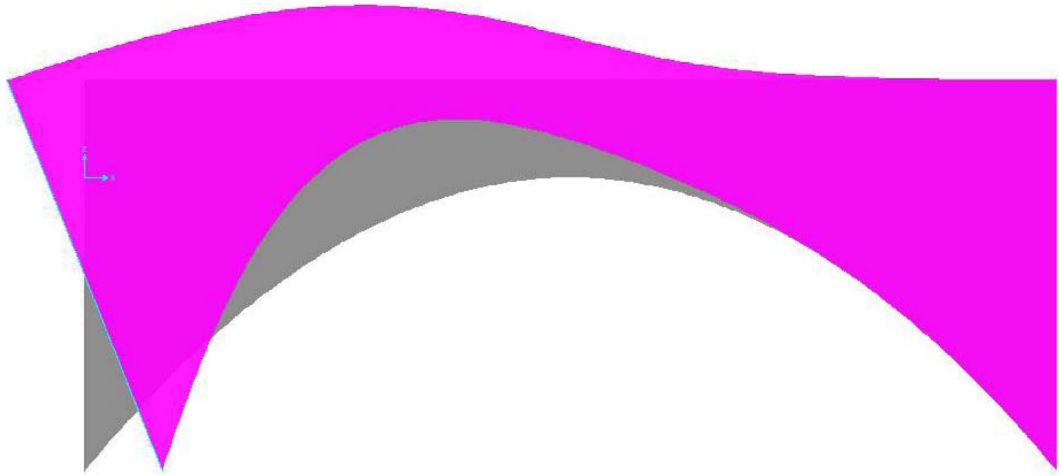
Fig. 12 Deformed shape of the 10 m long NBSPH for bending stiffness analyses

(a)   (b)
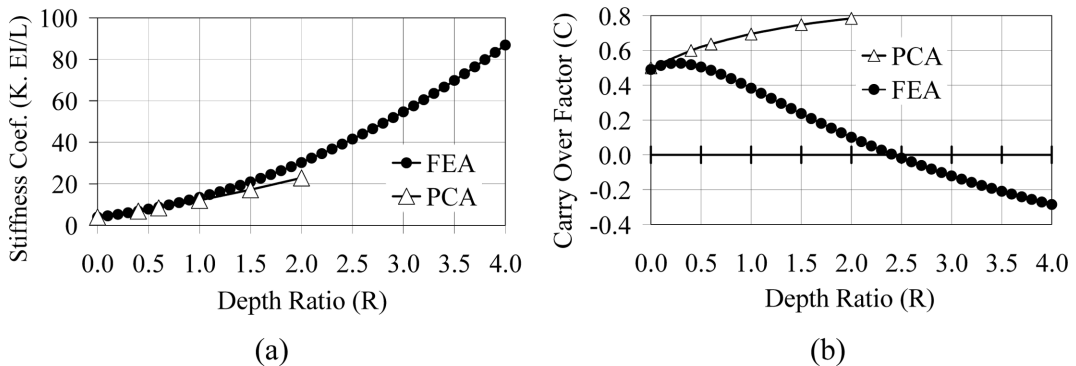
Fig. 13 Comparison of the values of (a) bending stiffness coefficients (K. EI/L), (b) carry-over factors (C) which were obtained from finite element analyses (FEA) with those of PCA (1958)

variation of the FEM_{OWN} values obtained from FEA. FEM_{OWN} values increase in a parabolic fashion as haunch depth ratios (R) are increased. Since the FEM_{OWN} values are not available in the PCA (1958), the FEM_{OWN} values obtained from the FEA could not be compared.

The bending stiffness and carry-over factors were obtained from the FEA. By definition, the bending stiffness of a beam element is the moment required to produce a unit rotation at one end while all other degrees of freedoms (d.o.f.s) are set to zero. The carry-over factor (C) is the ratio of the moment developed at the other end to the applied moment. In order to ensure the linear end rotations, a rigid frame element was attached to one end of the NBSPH as shown in Fig. 12. The end moments were calculated at the centroids of the end sections of the NBSPH. In FEA, the end rotations and unit displacements were represented by a set of prescribed nodal displacements. The deflected shape of 10 m long NBSPH due to unit rotation at the left end is illustrated in Fig. 12.

The results obtained from the FEA are compared with those of PCA (1958) for different haunch depth ratios. The comparisons of the plots for the bending stiffness coefficients [K = bending stiffness / (EI/L)] and the carry-over factors (C) are presented in Fig. 13(a) and Fig. 13(b),

respectively. The bending stiffness coefficients obtained by FEA were greater than those given in PCA (1958) for the NBSPH. The arching action increases the bending stiffness and therefore helps the NBSPH to resist against the rotation near the supports. Most importantly, there was a strong coupling between the bending moments and the axial forces. The axial forces developed in restrained NBSPH due to arching action tended to counteract the carried over moment. This factor causes reduction on the carry-over factor obtained by FEA. This explains the large deviation in carry-over factors for the NBSPH having deep haunches.

From the above discussion it can be concluded that the fixed-end reactions, the stiffness coefficients and the carry-over factors given in PCA (1958) publications are in significant error especially for the members with deep haunches. It is concluded that the deviations reached to unacceptable levels for non-prismatic beams having deep haunches. The FEMs in PCA (1958) are generally over-estimated that the stiffness coefficients and the carry-over factors of the beam theories of PCA (1958) do not satisfy the bending stiffness and the carry-over factors due to unrestrained axial deformation. The results obtained from the FEA represent the correct ones and should be used in practice. However, if the member stiffness matrix is to be formed using K and C factors obtained from FEA, the coupling with axial forces must be considered.

6. Design formulas and the dimensionless design coefficients

The design equations and the dimensionless estimation coefficients were developed based on the results of the extensive parametric FEA with respect to the geometry of the NBSPH. The separate design equations were proposed for the calculation of the fixed-end reactions due to the uniformly distributed vertical loads (Eqs. (1) and (2)) the point loads at the mid-span (Eqs. (3) and (4)), the point loads $0.3 \times L$ from the left end of the NBSPH (Eqs. (5), (6) and (7)), the point loads $0.1 \times L$ from the left end of the NBSPH (Eqs. (8), (9) and (10)) and the self weights of the NBSPH (Eqs. (11) and (12)).

Separate design equations were proposed to be able to calculate the FEFs and FEMs of the NBSPH. The values of dimensionless estimation coefficients in Eqs. (1) to (12) were proposed in Table 1 and Table 2 for different haunch depth ratios (R). The proposed Eqs. (1) through (12) can be used to obtain more rigorous estimations for the fixed-end reactions of the NBSPH due to vertical loadings without necessitating FEA. In this paper, all the estimation coefficients are dimensionless and were obtained using the FEA. The developed equations for the direct evaluation of the design forces are as follows.

The fixed-end horizontal forces (FEF_W) and the fixed-end moments (FEM_W) at the centroids of the end sections of the NBSPH due to uniformly distributed vertical loadings are given in Eq. (1) and Eq. (2), respectively

$$\text{FEF}_W = \text{FC}_{(W)} \times w \times L \tag{1}$$

$$\text{FEM}_W = \text{MC}_{(W)} \times w \times L^2 \tag{2}$$

where L is the span length and w is the uniformly distributed vertical load. $\text{FC}_{(W)}$ and $\text{MC}_{(W)}$ are the estimator coefficients for calculating the FEF_W and FEM_W, respectively. The values of $\text{FC}_{(W)}$ and $\text{MC}_{(W)}$ are given in the second and third columns of Table 1, respectively.

Table 1 The values of the estimator coefficients of $FC_{(W)}$, $MC_{(W)}$, $FC_{(0.5L-P)}$, $MC_{(0.5L-P)}$, $FC_{(0.3L-P)}$, $MC_{(0.3L-P-L)}$ and $MC_{(0.3L-P-R)}$

R	$FC_{(W)}$	$MC_{(W)}$	$FC_{(0.5L-P)}$	$MC_{(0.5L-P)}$	$FC_{(0.3L-P)}$	$MC_{(0.3L-P-L)}$	$MC_{(0.3L-P-R)}$
0.0	0.0000	0.0836	0.0000	0.1242	0.0000	0.1456	0.0642
0.2	0.1267	0.0887	0.2173	0.1346	0.1520	0.1581	0.0651
0.4	0.1847	0.0913	0.3490	0.1398	0.2343	0.1667	0.0633
0.5	0.2045	0.0920	0.3953	0.1413	0.2608	0.1700	0.0619
0.6	0.2217	0.0924	0.4321	0.1422	0.2804	0.1728	0.0602
0.8	0.2408	0.0927	0.4842	0.1427	0.3047	0.1772	0.0565
1.0	0.2517	0.0923	0.5167	0.1420	0.3160	0.1804	0.0525
1.2	0.2566	0.0917	0.5381	0.1404	0.3195	0.1829	0.0485
1.4	0.2578	0.0908	0.5482	0.1384	0.3183	0.1848	0.0446
1.5	0.2575	0.0903	0.5519	0.1372	0.3165	0.1855	0.0428
1.6	0.2568	0.0897	0.5545	0.1359	0.3142	0.1862	0.0409
1.8	0.2543	0.0886	0.5571	0.1332	0.3088	0.1872	0.0374
2.0	0.2513	0.0874	0.5573	0.1303	0.3025	0.1880	0.0341
2.2	0.2476	0.0862	0.5559	0.1272	0.2958	0.1886	0.0310
2.4	0.2438	0.0850	0.5535	0.1241	0.2890	0.1890	0.0280
2.5	0.2419	0.0844	0.5520	0.1224	0.2856	0.1891	0.0266
2.6	0.2399	0.0838	0.5503	0.1208	0.2822	0.1892	0.0252
2.8	0.2360	0.0825	0.5467	0.1175	0.2757	0.1893	0.0226
3.0	0.2323	0.0813	0.5429	0.1142	0.2694	0.1892	0.0201
3.2	0.2286	0.0800	0.5388	0.1108	0.2634	0.1891	0.0178
3.4	0.2250	0.0788	0.5347	0.1074	0.2576	0.1889	0.0155
3.5	0.2233	0.0782	0.5326	0.1057	0.2549	0.1888	0.0144
3.6	0.2216	0.0776	0.5306	0.1040	0.2522	0.1886	0.0133
3.8	0.2184	0.0763	0.5265	0.1005	0.2470	0.1883	0.0113
4.0	0.2152	0.0751	0.5225	0.0971	0.2421	0.1879	0.0093

The fixed-end horizontal forces ($FEF_{0.5L-P}$) and the fixed-end moments ($FEM_{0.5L-P}$) at the centroids of the end sections of the NBSPH due to point loads at the mid-span are given in Eq. (3) and Eq. (4), respectively

$$FEF_{0.5L-P} = FC_{(0.5L-P)} \times P \times L \tag{3}$$

$$FEM_{0.5L-P} = MC_{(0.5L-P)} \times P \times L \tag{4}$$

where P is the vertical point load at the mid-span of the NBSPH. $FC_{(0.5L-P)}$ and $MC_{(0.5L-P)}$ are the estimator coefficients for calculating the $FEF_{0.5L-P}$ and the $FEM_{0.5L-P}$, respectively. The values of $FC_{(0.5L-P)}$ and $MC_{(0.5L-P)}$ are given in the fourth and fifth columns of Table 1, respectively.

The fixed-end horizontal forces ($FEF_{0.3L-P}$) at the centroids of the end sections, the fixed-end moments at the centroid of the left end ($FEM_{0.3L-P-L}$) and the fixed-end moments at the centroid of the right end ($FEM_{0.3L-P-R}$) due to the point load at $0.3 \times L$ from the left end of the NBSPH are

Table 2 The values of the estimator coefficients of $FC_{(0.1L-P)}$, $MC_{(0.1L-P-L)}$, $MC_{(0.1L-P-R)}$, $FC_{(OWN)}$, $MC_{(OWN)}$, stiffness coefficients (K) and carry-over factors (C)

R	$FC_{(0.1L-P)}$	$MC_{(0.1L-P-L)}$	$MC_{(0.1L-P-R)}$	$FC_{(OWN)}$	$MC_{(OWN)}$	K	C
0.0	0.0101	0.0795	0.0102	0.0000	0.0834	3.925	0.490
0.2	0.0356	0.0825	0.0094	0.1107	0.0920	5.277	0.524
0.4	0.0475	0.0844	0.0084	0.1804	0.0983	6.893	0.518
0.5	0.0505	0.0851	0.0079	0.2047	0.1009	7.805	0.504
0.6	0.0524	0.0856	0.0074	0.2239	0.1032	8.787	0.485
0.8	0.0538	0.0864	0.0065	0.2510	0.1072	10.967	0.438
1.0	0.0538	0.0868	0.0061	0.2676	0.1106	13.439	0.382
1.2	0.0535	0.0870	0.0057	0.2777	0.1135	16.207	0.324
1.4	0.0522	0.0874	0.0049	0.2835	0.1163	19.273	0.266
1.5	0.0507	0.0877	0.0043	0.2853	0.1176	20.918	0.237
1.6	0.0498	0.0878	0.0040	0.2865	0.1189	22.638	0.208
1.8	0.0489	0.0878	0.0037	0.2878	0.1213	26.304	0.153
2.0	0.0472	0.0880	0.0032	0.2878	0.1237	30.271	0.101
2.2	0.0456	0.0880	0.0027	0.2871	0.1260	34.541	0.051
2.4	0.0439	0.0880	0.0023	0.2859	0.1283	39.114	0.004
2.5	0.0426	0.0880	0.0019	0.2852	0.1294	41.515	-0.019
2.6	0.0419	0.0880	0.0017	0.2845	0.1305	43.993	-0.041
2.8	0.0413	0.0880	0.0016	0.2828	0.1327	49.179	-0.082
3.0	0.0400	0.0879	0.0012	0.2811	0.1349	54.675	-0.121
3.2	0.0388	0.0878	0.0009	0.2793	0.1370	60.482	-0.158
3.4	0.0378	0.0878	0.0007	0.2775	0.1392	66.602	-0.193
3.5	0.0368	0.0877	0.0004	0.2767	0.1402	69.781	-0.210
3.6	0.0364	0.0876	0.0003	0.2758	0.1413	73.038	-0.226
3.8	0.0359	0.0875	0.0001	0.2741	0.1434	79.787	-0.257
4.0	0.0351	0.0874	-0.0001	0.2725	0.1455	86.849	-0.286

given in Eq. (5), Eq. (6) and Eq. (7), respectively

$$FEF_{0.1L-P} = FC_{(0.1L-P)}, \times P \times L \qquad (5)$$

$$FEM_{0.3L-P-L} = MC_{(0.3L-P-L)} \times P \times L \qquad (6)$$

$$FEM_{0.3L-P-R} = MC_{(0.3L-P-R)} \times P \times L \qquad (7)$$

where P is the vertical point load at $0.3 \times L$ from the left end of the NBSPH. $FC_{(0.3L-P)}$, $MC_{(0.3L-P-L)}$ and $MC_{(0.3L-P-R)}$ are the estimator coefficients for calculating the $FEF_{0.3L-P}$, $FEM_{0.3L-P-L}$ and $FEM_{0.3L-P-R}$, respectively. The values of $FC_{(0.3L-P)}$, $MC_{(0.3L-P-L)}$, and $MC_{(0.3L-P-R)}$ are given in the sixth, seventh and eighth columns of Table 1, respectively.

The fixed-end horizontal forces ($FEF_{0.1L-P}$) at the centroids of the end sections, the fixed-end moments at the centroid of the left end ($FEM_{0.1L-P-L}$) and the fixed-end moments at the centroid of the right end ($FEM_{0.1L-P-R}$) due to the point load at $0.1 \times L$ from the left end of the NBSPH are

given in Eq. (8), Eq. (9) and Eq. (10), respectively

$$\text{FEF}_{0.1L\text{-}P} = \text{FC}_{(0.1L\text{-}P)} \times P \times L \tag{8}$$

$$\text{FEM}_{0.1L\text{-}P\text{-}L} = \text{MC}_{(0.1L\text{-}P\text{-}L)} \times P \times L \tag{9}$$

$$\text{FEM}_{0.1L\text{-}P\text{-}R} = \text{MC}_{(0.1L\text{-}P\text{-}R)} \times P \times L \tag{10}$$

where P is the vertical point load at $0.1 \times L$ from the left end of the NBSPH. $\text{FC}_{(0.1L\text{-}P)}$, $\text{MC}_{(0.1L\text{-}P\text{-}L)}$ and $\text{MC}_{(0.1L\text{-}P\text{-}R)}$ are the estimator coefficients for calculating the $\text{FEF}_{0.1L\text{-}P}$, $\text{FEM}_{0.1L\text{-}P\text{-}L}$, and $\text{FEM}_{0.1L\text{-}P\text{-}R}$, respectively. The values of $\text{FC}_{(0.1L\text{-}P)}$, $\text{MC}_{(0.1L\text{-}P\text{-}L)}$, and $\text{MC}_{(0.1L\text{-}P\text{-}R)}$ are given in the second, third and fourth columns of Table 2, respectively.

The fixed-end horizontal forces (FEF_{OWN}) and the fixed-end moments (FEM_{OWN}) at the centroids of the end sections of the NBSPH due its self weight of the NBSPH are given in Eq. (11) and Eq. (12), respectively.

$$\text{FEF}_{\text{OWN}} = \text{FC}_{(\text{OWN})} \times (\gamma \times b \times h) \times L \tag{11}$$

$$\text{FEM}_{\text{OWN}} = \text{MC}_{(\text{OWN})} \times (\gamma \times b \times h) \times L^2 \tag{12}$$

where γ is the unit weight of the material, L is the span length, b is the width, h is the mid-span depth or minimum depth of NBSPH. $\text{FC}_{(\text{OWN})}$ and $\text{MC}_{(\text{OWN})}$ are the estimator coefficients for calculating the FEF_{OWN} and FEM_{OWN}, respectively. The values of $\text{FC}_{(\text{OWN})}$ and $\text{MC}_{(\text{OWN})}$ are given in the fifth and sixth columns of Table 2, respectively.

The values of bending stiffness coefficients (K) and the carry-over factors (C) obtained from the FEA are presented in the seventh and eighth columns of Table 2, respectively. The fixed-end reactions, stiffness coefficients and carry-over factors are changed depending on the haunch depths. Since the cross-sectional dimensions affect the behavior of the non-prismatic beams with parabolic haunches, thus, they are important in the arch formation and affect the location of arch height and, in turn, affect the axial thrust values, fixed-end reactions, stiffness coefficients and carry-over factors. The formulations and estimation coefficients presented in this paper take into account the dimensions of the rectangular cross-section of the NBSPH, the discontinuity of the centroidal axis, the local stress concentrations, the nonlinear stress distributions and the existence of the null areas that reduces the member stiffness.

7. Conclusions

In this paper, the linear elastic behavior of the NBSPH subjected to vertical loading conditions was investigated using plane stress FEA considering the thrust effects. The parametric studies were performed for the NBSPH with $b = 0.5$ m, $h = 1.0$ m, $L = 10$ m and having haunch depth ratios (R) varying in the range of 0.0 to 4.0 with 0.1 intervals and for the haunch length ratio of $\alpha = 0.5$. An extensive parametric study was conducted and the fixed-end reactions, stiffness coefficients and carry-over factors were computed using the realistic theoretical models. Based on the results of FEA, the design formulas (Eqs. (1)-(12)) and the design coefficients (Tables 1, 2) were proposed to be able to compute the fixed-end reactions, stiffness coefficients and carry-over factors without necessitating any additional FEA. The proposed formulas and dimensionless estimation coefficients were expressed in simplified forms, so that they are directly applicable in analyzing and re-

evaluation of the NBSPH. The dimensionless estimation coefficients were separately proposed as the functions of the haunch depth ratios. It should be pointed out that, although the presented results are valid only for the non-prismatic beams having symmetrical parabolic haunches and the haunch length ratio of $\alpha = 0.5$, the approach can easily be expanded to cover the other types of non-prismatic beams. Also, it should be pointed out that the proposed dimensionless estimation coefficients are only valid for the NBSPH having fixed-end conditions.

The FEA results obtained from this study were compared with those available in the literature. The comparison of the fixed-end reactions, stiffness coefficients and carry-over factors of NBSPH members available in the literature with those computed by FEA revealed large discrepancies. It is determined that the conventional analysis methods using beam theories for these types of structures led to erroneous results where the major source of error was the neglection of the continuous changes of the centroidal axis resulting in neglecting the coupling between the axial forces and the bending moments. Due to progressive change associated with the non-prismatic section of the NBSPH, a considerable amount of FEFs initiated in addition to FEMs under vertical loading condition. The resulting FEFs are significantly important for NBSPH especially having deep haunches. Since NBSPH behave similar to archs, this behavior becomes more pronounced as the haunch depth ratios increase. Unless a detailed FEA is utilized, the conventional methods using frame elements become deficient to compute such FEFs due to the progressive change in the centroidal axis of the non-prismatic section. The authors recommend using the FEA results considering the coupling effect completely as well as stress distributions rather than using tables by PCA (1958) or conventional analysis method with large deviations, as shown in this study.

Acknowledgements

References

Al-Gahtani, H.J. (1996), "Exact stiffnesses for tapered members", *J. Struct. Eng.-ASCE,* **122**(10), 1234-1239.
Balkaya, C. (2001), "Behavior and modeling of nonprismatic members having T-sections", *J. Struct. Eng.-ASCE,* **127**(8), 940-946.
Balkaya, C., Kalkan, E. and Yuksel, S.B. (2006), "FE analysis and practical modeling of RC multi-bin circular silos", *ACI Struct. J.,* **103**(3), 365-371.
Bathe, K.J. (1996), *Finite Element Procedures*, Prentice Hall Publisher, NJ, USA.
Brown, C.J. (1984), "Approximate stiffness matrix for tapered beams", *J. Struct. Eng.-ASCE,* **110**(12), 3050-3055.
CSI (2007), Computer and Structures Inc., SAP2000 User's Manual, Berkeley, CA.
Eisenberger, M. (1985), "Explicit stiffness matrices for non-prismatic members", *Comput. Struct.,* **20**(4), 715-720.
Eisenberger, M. (1991), "Stiffness matrices for non-prismatic members including transverse shear", *Comput. Struct.,* **40**(4), 831-835.
El-Mezaini, N., Balkaya, C. and Citipitioglu, E. (1991), "Analysis of frames with nonprismatic members", *J. Struct. Eng.-ASCE.,* **117**(6), 1573-1592.
Friedman, Z. and Kosmatka, J.B. (1992a), "Exact stiffness matrix of a non-uniform beam-I. Extension, torsion, and bending of a Bernoulli-Euler beam", *Comput. Struct.,* **42**(5), 671-682.

Friedman, Z. and Kosmatka, J.B. (1992b), "Exact stiffness matrix of a non-uniform beam-II. Bending of a Timoshenko beam", *Comput. Struct.,* **49**(3), 545-555.

Funk, R.R. and Wang, K.T. (1988), "Stiffness of non-prismatic members", *J. Struct. Eng.-ASCE,* **114**(2), 489-494.

Hibbeler, R. (2002), *Structural Analysis,* NJ: Prentice-Hall, Inc., Fifth Edition, Upper Saddle River, New Jersey.

Horrowitz, B. (1997), "Singularities in elastic finite element analysis", *Concrete Int.,* December, 33-36.

Maugh, L.C. (1964), *Statically Indeterminate Structures: Continuous Girders and Frames with Variable Moment of Inertia*, John & Wiley, New York.

Medwadowski, S.J. (1984), "Nonprismatic shear beams", *J. Struct. Eng.-ASCE,* **110**(5), 1067-1082.

Portland Cement Association (PCA) (1958), *Beam Factors and Moment Coefficients for Members of Variable Cross-section*, Handbook of Frame Constants, Chicago.

Tartaglione, L.C. (1991), *Structural Analysis*, McGraw-Hill, Ins, United States of America.

Tena-Colunga, A. (1996), "Stiffness formulation for nonprismatic beam elements", *J. Struct. Eng.-ASCE,* **122**(12), 1484-1489.

Timoshenko, S.P. and Young, D.H. (1965), *Theory of Structures*, McGraw-Hill Book Co., Inc., New York, USA.

Valderbilt, M.D. (1978), "Fixed-end action and stiffness matrices for non-prismatic beams", *ACI Struct. J.,* **75**(1), 290-298.

Weaver, W. and Gere, J.M. (1990), *Matrix Analysis of Framed Structures*, Van Nostrand Reinhold, New York.

Yuksel, S.B. (2008), "Slit connected coupling beams for tunnel form building structures", *Struct. Des. Tall Spec. Build.,* **17**(3), 579-600.

Yuksel S.B. (2009a), "Behaviour of symmetrically haunched non-prismatic members subjected to temperature changes", *Struct. Eng. Mech.*, **31**(3), 297-314.

Yüksel, S.B. (2009b), "Investigation of the behavior of single span reinforced concrete historic bridges by using finite element method", *Proceedings of the Eleventh International Conference on Structural Repairs and Maintenance of Heritage Architecture (STREMAH 2009)*, Tallinn, Estonia, July.

Yüksel, S.B. (2009c), "Investigation of the behavior of single span reinforced concrete historic bridges by using finite element method", Report No. TÜBİTAK-MAG-107M639, Scientific and Technical Research Council of Turkey. (in Turkish)

Yuksel, S.B. and Arikan, S. (2009), "A new set of design aids for the groups of four cylindrical silos due to interstice and internal loadings", *Struct. Des. Tall Spec. Build.,* **18**(2), 149-169.

Notations

The following symbols are used in this paper:

E = modulus of elasticity of the material;

FEF = fixed-end horizontal forces at the centroids of the end sections of the NBSPH due to vertical loadings;

FEM = fixed-end moments at the centroids of the end sections of the NBSPH due due to vertical loadings;

FEF_W = fixed-end horizontal forces at the centroids of the end sections of the NBSPH due to uniformly distributed vertical loads;

$FEF_{0.5L-P}$ = fixed-end horizontal forces at the centroids of the end sections of the NBSPH due to point loads at the mid-span;

$FEF_{0.3L-P}$ = fixed-end horizontal forces at the centroids of the end sections of the NBSPH due to the point load at $0.3 \times L$ from the left end;

$FEF_{0.1L-P}$ = fixed-end horizontal forces at the centroids of the end sections of the NBSPH due to the point load at $0.1 \times L$ from the left end;

FEF_{OWN} = fixed-end horizontal forces at the centroids of the end sections of the NBSPH due to its own weight;

$FC_{(W)}$ = dimensionless coefficients for calculating the FEF_W;

$FC_{(0.5L-P)}$ = dimensionless coefficients for calculating the $FEF_{0.5L-P}$;

$FC_{(0.3L-P)}$ = dimensionless coefficients for calculating the $FEF_{0.3L-P}$;

$FC_{(0.1L-P)}$ = dimensionless coefficients for calculating the $FEF_{0.1L-P}$;

FEM_W = fixed-end moments at the centroids of the end sections of the NBSPH due to uniformly distributed vertical load;

$FEM_{0.5L-P}$ = fixed-end moments at the centroids of the end sections of the NBSPH due to the point loads at the mid-span;

$FEM_{0.3L-P-L}$ = fixed-end moment at the centroid of the left end of the NBSPH due to the point load at $0.3 \times L$ from the left end;

$FEM_{0.3L-P-R}$ = fixed-end moment at the centroid of the right end of the NBSPH due to the point load at $0.3 \times L$ from the left end;

$FEM_{0.1L-P-L}$ = fixed-end moment at the centroid of the left end of the NBSPH due to the point load at $0.1 \times L$ from the left end;

$FEM_{0.1L-P-R}$ = fixed-end moment at the centroid of the right end of the NBSPH due to the point load at $0.1 \times L$ from the left end;

FEM_{OWN} = fixed-end moments at the centroids of the end sections of the NBSPH due to its own weight;

$MC_{(W)}$ = dimensionless coefficients for calculating the FEM_W;

$MC_{(0.3L-P-L)}$ = dimensionless coefficients for calculating the fixed-end moments at the left end due to the point load at $0.3 \times L$ from the left end;

$MC_{(0.3L-P-R)}$ = dimensionless coefficients for calculating the fixed-end moments at the right end due to the point load at $0.3 \times L$ from the left end;

$MC_{(0.3L-P- RIGHT)}$= dimensionless coefficients for calculating the fixed-end moments at the right end at the left end due to the point load at $0.3 \times L$ from the left end;

$MC_{(0.1L-P-LEFT)}$ = dimensionless coefficients for calculating the fixed-end moments at the left end due to the point load at $0.1 \times L$ from the left end;

$MC_{(0.3L-P- RIGHT)}$= dimensionless coefficients for calculating the fixed-end moments at the right end at the right end due to the point load at $0.1 \times L$ from the left end;

γ = is the unit weight of the material;

h = mid-span depth or smallest depth of the non-prismatic element;

R = the haunch depth ratio;

α = the haunch length ratio (haunch length divided by the total length of the member);

v = Poisson's Ratio of the material;

E = modulus of elasticity of the material;
b = width of the member;
w = uniformly distributed vertical load at the top face of the NBHSP;
L = span length of the NBHSP;
P = vertical point load at the top surface of the NBHSP;
K = bending stiffness coefficients [Bending stiffness / (EI/L)];
C = carry-over factors